Part IV
Microstructured Devices for Purification and Separation Processes

12
Extraction

Nobuaki Aoki and Kazuhiro Mae

12.1
Introduction

In miniaturized channels of microstructured devices, a high surface area to volume ratio leads to enhanced mass transfer between two immiscible phases such as water and oil. Extraction is one of the unit operations for separation using mass transfer between two liquid phases and is often used for the separation of compounds in which the difference in boiling points is small. Several microstructured devices for efficient extraction have been developed. In this chapter, microstructured devices for extraction are introduced with divided into the following three categories according to fluid operations:

1. parallel flow of two immiscible phases
2. droplet manipulation
3. slug flow.

The separation operation is essential for the reaction process. Extended uses of microstructured devices for extraction in organic syntheses are also discussed.

12.2
Parallel Flow of Two Immiscible Phases

Miniaturized channels of the order of hundreds of micrometers, as shown in Figure 12.1, are simple and common microstructured devices for extraction. In the main channel, the fluids of the two phases flow parallel in the axial direction. The extraction using this flow pattern leverages the reduction in diffusion length between two immiscible fluids through miniaturization, since the diffusive mass transfer time scales with the square of this length. Thus, reducing the channel size enhances the extraction efficiency in these devices. In addition to an improved mass transfer rate, the two phases separate at the branched outlet of the main channel, which omits the operation for phase separation and permits further operation by connecting

Micro Process Engineering, Vol.1: Fundamentals, Operations and Catalysts
Edited by V. Hessel, A. Renken, J.C. Schouten, and J.-I. Yoshida

ISBN: 978-3-527-31550-5

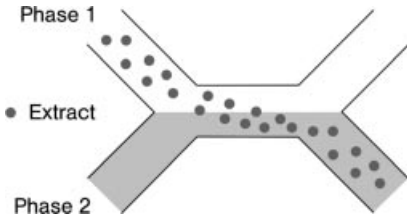

Figure 12.1 Microchannel for extraction based on parallel flow of immiscible fluids.

additional channels. In these devices, for extending the operating conditions forming stable parallel flow, the effects of channel surface modification using a hydrophobic group and its geometry for the part in which interface is formed on extraction efficiency are often investigated.

12.2.1 Instances of Extraction Systems and Devices Using Parallel Flow

Minagawa *et al.* performed the extraction of a metal cation in the form of a chelate using a microchip comprising two Y-shaped confluence zones and a branched outlet [1]. Co(II) is extracted into *m*-xylene from aqueous solution as 2-nitroso-1-naphthol chelates and colorimetric determination of the *m*-xylene phase is applied by a thermal lens microscope (TLM) as shown in Figure 12.2. The microchannels are 250 μm wide and 100 μm deep. The length of a reaction for forming chelate and solvent extraction is 5 mm. The time for extraction in the channel is 10 min, which is about one order of magnitude shorter than that for a conventional system using a separating funnel and mechanical shaker.

Kuban *et al.* carried out the extraction of Methylene Blue (MB) in an aqueous phase into butanol using ion pairs in a microchannel [2]. The extraction efficiency of MB into hexanol is poor, but in the presence of an anionic surfactant such as dodecylbenzenesulfonic acid (DBSA), an ion pair MB^+–$DBSA^-$ is formed that is easily extracted. Figure 12.3 shows the device constructed from two glass slides (GS1 and GS2). The channel length for extraction is 45 mm. The flow channel between the two glass slides was formed by a three-layer spacer and its depth can be changed from 150

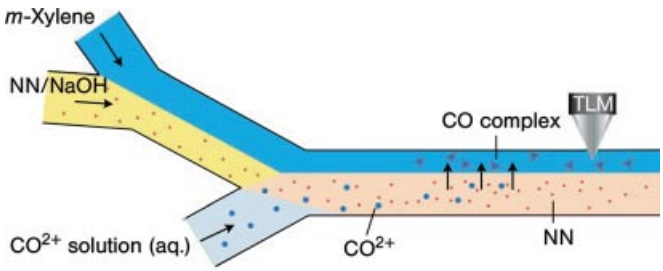

Figure 12.2 Microchannel for the extraction of Co(II) in the form of a chelate. Reproduced by permission of the Royal Society of Chemistry [1].

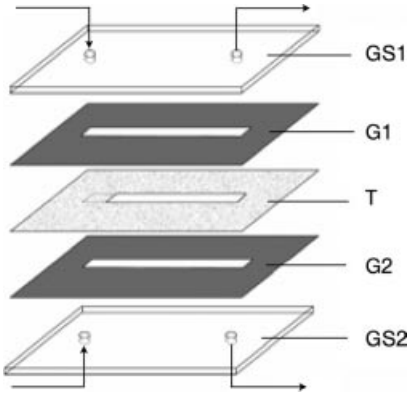

Figure 12.3 Schematic of microchannel device for ion pair solvent extraction. Reproduced by permission of the American Chemical Society [2].

to 380 μm. Either black electric tape (thickness 150 μm) or Kapton polyimide tape (thickness 80 or 50 μm) is used for the outer gaskets G1 and G2 and defined the boundaries of the flow channel. The intermediate gasket T is made from a polyester transparency sheet (thickness 50 or 80 μm).

Kitamori's group also performed an extraction of aqueous phase Fe(II) into chloroform using the ion pair Fe–bathophenanthroline disulfonic acid complex, in a X-shaped microchannel fabricated in a quartz glass chip [3]. The microchannels are 250 μm wide and 100 μm deep. The glass chip has a solvent extraction region of length 10 mm. The time in this microchannel, 45 s, roughly coincides with the molecular diffusion time. The same group also performed ionophore-based ion pair extraction of K^+ and Na^+ in an aqueous phase into butyl acetate using a Y-shaped channel 10 mm long, 100 μm deep and 250 μm wide [4]. The device material was quartz glass. The sodium ionophore was 2,6,13,16,19-pentaoxapentacyclo [18.4.4.4.^{7,12}0.^{1,20}0^{7,12}]dotriacontane (DD16C5) and the potassium ionophore was dibenzo-18-crown-6 (DB18C6).

Other instances of extraction based on parallel flow using simple X- or Y-shaped channels are summarized in Table 12.1 [5–9].

Extraction devices using parallel flow combined with a membrane have also been developed. The fluids of two immiscible phases are separated by a membrane. Cai *et al.* performed extraction of butyl Rhodamine B (BRB) in aqueous solution into isobutanol. Polytetrafluoroethylene (PTFE) membranes with different pore sizes of 0.2, 0.45 and 1.0 μm (60 μm thick, 70–80% porosity) was placed between the two phases [10]. Aqueous flow rates in the range 22–65 μL min^{-1} were investigated with a solvent flow-rate of 8.2 zμL min^{-1}. The extraction efficiency improves with increasing membrane pore size and aqueous flow rate.

Wang *et al.* developed an extraction device with a Celgard 2400 microporous polypropylene membrane [11]. It has an average thickness of 25 μm, the pore size is 0.05 μm and 38% of the surface is porous. The channel is made of polycarbonate and

Table 12.1 Instances of extraction systems and devices based on parallel flow.

Ref.	Extraction system	Channel geometry and material	Extraction time (s)
5	Progesterone and 11α-hydroxy-progesterone in aqueous phase into ethyl acetate	X-shape, width 220 μm, depth 50 μm, length 332 mm, glass	
6	Hydrocarbon fraction from oil into hexane	X-shape, width 700 μm, glass	2.4–4.8
7	U(VI) from aqueous phase into tri-*n*-butyl phosphate	X-shape, width 100.5 μm, depth 43.5 μm, length 120 mm, Pyrex glass	1
8	Al^{3+}-DHAB(2,2′-dihydroxyazo-benzene) chelate from water into 1-butanol (BuOH)	Y-shape, width 200 μm, depth 10 μm, styrol	8
9	Co–2-nitroso-5-dimethylamino-phenol complex in aqueous phase into toluene	X-shape, width 250 μm, depth 100 μm, 2 mm long, glass	60

its widths are 750 and 1000 μm. Using this device, extraction of haloacetic acid in an aqueous phase into acetonitrile was carried out.

Multilayer parallel flows can also be formed in microstructured devices and increase the interfacial area, allowing efficient extraction. Hibara *et al.* had developed a device for three-layer flow [12]. The inlet of the device is branched into three ways. A water–ethyl acetate–water interface is formed in a 70 μm wide and 30 μm deep channel (Pyrex glass). The interface is stable and maintained for a distance of more than 18 cm. As an example of application, the liquid–liquid extraction of a codi-methylaminophenol complex in the microchannel was performed. The solvent extraction process of the complex into *m*-xylene in the multilayer flow was found to reach equilibrium in 4 s, whereas it took 60 s in a simple two-phase extraction.

The three-layer flow is extended to rapid transport of analytes through an organic liquid membrane [13]. Figure 12.4 shows the experimental setup and a photograph of microchannels near the phase confluence point. In the continuous laminar flow

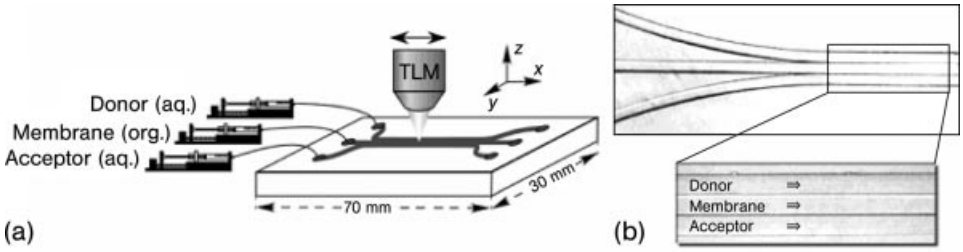

Figure 12.4 Schematic (a) and photograph (b) of the device for the transport of analyte through an organic liquid membrane. Reproduced by permission of the American Chemical Society [13].

region, the analyte (Methyl Red) is rapidly extracted across the microchannel from the donor to the acceptor phase through the organic solvent phase (cyclohexane). The thickness of the organic phase, sandwiched by the two aqueous phases, is ~64 μm and it is considered as a thin liquid organic membrane.

12.2.2 Surface Modification of Channel Geometry for Stabilizing Parallel Flow

For stabilizing parallel flow to extend the operating conditions and thus enhance the extraction efficiency, the microchannel surface is chemically modified. Hibara *et al.* [14] and Xiao *et al.* [15] modified the glass channel surface using octadecyltrichlorosilane (OTS). Only the surface with flowing organic phase is coated with OTS, and the channel surface for the aqueous phase is bare glass. Through this modification, the aqueous phase selectively flows in the channel without the OTS coating, and the organic phase with the coating.

Channel geometry also contributes to stabilization of the interface between immiscible fluids in parallel flow. Maruyama *et al.* carried out liquid–liquid extraction of metal ions in a microfluidic device with intermittent partition walls in the center of the confluent microchannel, 100 μm wide, 20 μm deep and 3 cm long [16]. The intermittent partition walls (50 mm long) stabilize a two-phase (*n*-heptane–water) flow and allow clear phase separation at the end-junction of the microchannel as shown in Figure 12.5. Although the apparent interfacial area in the microchannel is reduced by introducing the partition walls, the presence of the partition walls improved the extraction efficiency 2–3-fold at a contact time of 0.12–0.24 s. Flow analyses using fluorescent beads and a computational fluidic dynamics simulation indicated that a slight turbulence induced by the partition walls would result in the mixing of the aqueous phase and promote the transport of yttrium ions from the aqueous phase to the organic phase. Tagawa *et al.* also confirmed the effectiveness of an intermittent guide structure for enhancing the stability of a two phase interface and the product yield of a biphasic hydrolysis reaction of benzoyl chloride [17]. A channel for each phase with a bowl-shaped bottom is another device geometry that improves the stability of a two-phase interface [18, 19].

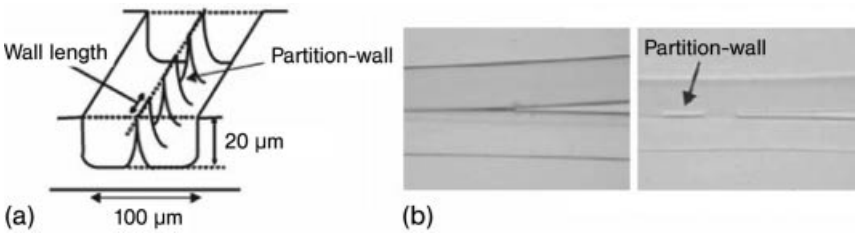

Figure 12.5 Schematic of microchannel with intermittent partition wall (a) and flow pattern near end-junction without (b) and with (c) partition wall. Reproduced by permission of the Royal Society of Chemistry [16].

12.2.3
Application in Organic Synthesis

Parallel flow of immiscible fluids with mass transfer between the two phases can also be used in phase-transfer synthetic reactions. This flow operation is useful for realizing reaction-controlling conditions for increasing the selectivity of desired products. As noted in [3], the mass transfer time in parallel flow corresponds to the molecular diffusion time and is proportional to W^2/D, where W is the diffusion length (m) and D is the diffusion coefficient ($m^2\,s^{-1}$). For instance, in a reaction system of a first-order reaction with a rate constant k (s^{-1}), the dimensionless number ϕ, representing the ratio of reaction rate to diffusive mixing rate, is denoted by $\phi = kW^2/D$. This number is called the Damköhler number [20]. To achieve reaction-controlling conditions, the value of ϕ should usually be less than the order of unity. When this criterion is satisfied by designing a channel, we can choose this flow pattern for phase-transfer synthetic reactions.

Hisamoto *et al.* demonstrated diazo coupling reaction shown in Figure 12.6 [21]. Maruyama *et al.* performed the degradation of *p*-chlorophenol using enzyme (laccase) solubilized in a succinic aqueous buffer [22]. In the former example, rapid phase transfer of starting material and the produced chemical species across the liquid–liquid interface play important roles in realizing both a fast chemical reaction and isolation of the produced chemical species. For the diazo coupling reaction, an undesirable side-reaction of the main product and a second diazonium salt to form a bisazo product is known [23]. Thus, in this reaction system, the large specific interfacial area and short molecular diffusion distance play important roles in removing the main product from the aqueous phase to the organic phase, which allows the undesirable side-reaction to be avoided.

Extraction devices with parallel flow have been integrated into reaction and separation systems [24–26]. Honda *et al.* [26] developed a microreaction system for the optical resolution of racemic amino acids. Figure 12.7 shows a schematic of the system. The microreactor used for the enzymatic reaction is a PTFE tube (500 mm inner diameter) with immobilized acylase on the inner wall. The channel for extraction has 200 μm width, 100 μm depth and 40 mm length and the space between plates is made of glass (bottom) and silicon (top). The channel surface of silicon is coated with Au and octadodecyl groups. Consequently, the resulting microchannel has a hydrophilic

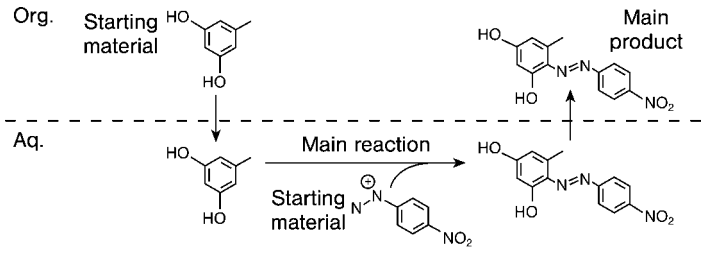

Figure 12.6 Phase transfer diazo coupling reaction. Reproduced by permission of the Royal Society of Chemistry [21].

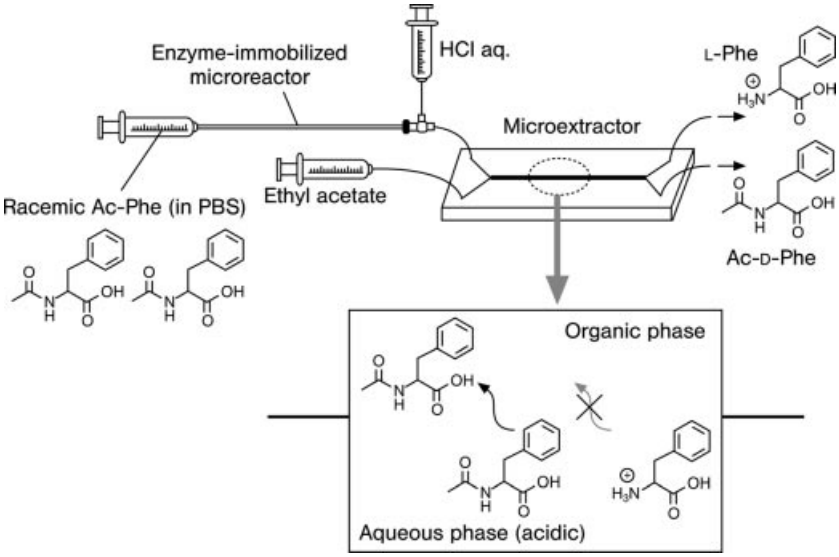

Figure 12.7 Continuous flow system for enantioselective separation of racemic amino acids. Reproduced by permission of the Royal Society of Chemistry [26].

surface on the lower side and a hydrophobic surface on the upper side. Racemic acetyl-D,L-amino acid (*N*-acetyl-D,L-phenylalanine, abbreviated as racemic Ac-Phe in Figure 12.7) is hydrolyzed enantioselectively in the enzyme-immobilized microreactor to give the L-amino acid (L-phenylalanine, abbreviated as L-Phe) and the unhydrolyzed acetyl-D-amino acid. Then, the aqueous reaction mixture is acidified by addition of HCl. The acetyl-D-amino acid (*N*-acetyl-D-phenylalanine, Ac-D-Phe) loses its charge and increases its ethyl acetate solubility. Subsequently, the resultant aqueous solution forms a laminar flow with ethyl acetate in the microextractor. The L-amino acid and acetyl-D-amino acid are thereby separated through the interface of the laminar flow on the basis of their different solubilities in ethyl acetate. Use of the enzyme microreactor permitted a highly enantioselective reaction for a racemic amino acid derivative. The microextractor provided a laminar flow of two immiscible solutions, which allowed selective extraction of the product. Using this integrated device, efficient continuous production of optically pure unnatural amino acids can be achieved.

12.3 Droplet Manipulation

An emulsion is a biphasic solution including dispersed small oil droplets in an aqueous phase. Because of the small channel size and high fluid velocity in micromixers, high shear force is applied to fluids, resulting in the generation of an emulsion in addition to enhancement of the mixing performance. The emulsion produced using micromixers has the characteristics of stability without surfactant,

small size and narrow size distribution. The large interfacial area between the oil and water phases leading to a short diffusion path of the extract and a high throughput of emulsion by micromixers provide an efficient extraction process. However, the stability of the emulsion also leads to a difficulty in the separation of the two phases after extraction. To overcome this disadvantage, devices to coalesce droplets have been developed. In this section, we also introduce devices for the individual manipulation of droplets for the system requiring precise operation of each droplet.

12.3.1 Devices for Continuous Generation of Dispersed Droplets

Multilamination mixers such as the IMM interdigital mixer and SuperFocus mixer have been used for generating emulsions and extraction based on emulsions [27–29]. For the IMM mixer, the emulsion diameter decreases linearly with increase in the total volume flow rate of two phases. For a system of silicone oil–water with a feed ratio of 1:1 using a 30-channel interdigital mixer, the diameter reaches less than 10 μm at a total volume flow rate of 1200 mL^{-1}. The extraction efficiency has a maximum at intermediate to high flow rates and decreases again at very high flow rates.

Mae *et al.* proposed a micromixer based on repeated splitting and recombination and demonstrated its application for extraction using an emulsion (abbreviated as YM-1) [30]. A soap-free emulsion with a diameter of the order of 1 μm can be produced in a short contact time of 0.1 s. The maximum production capacity of a single mixer is 200 $t\,yr^{-1}$, which is sufficient for the industrial production of fine chemicals and pharmaceutical compounds. Figure 12.8 shows the results for the extraction of phenol from dodecane into water using the YM-1 and an IMM mixer.

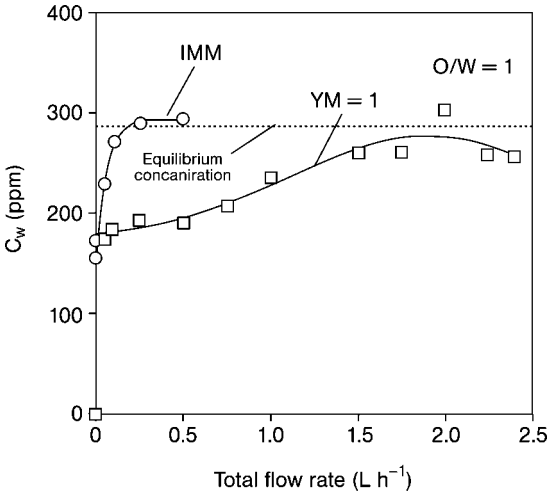

Figure 12.8 Effect of total flow rate on the extraction yield of phenol for YM-1 and IMM mixers. Reproduced by permission of Elsevier [30].

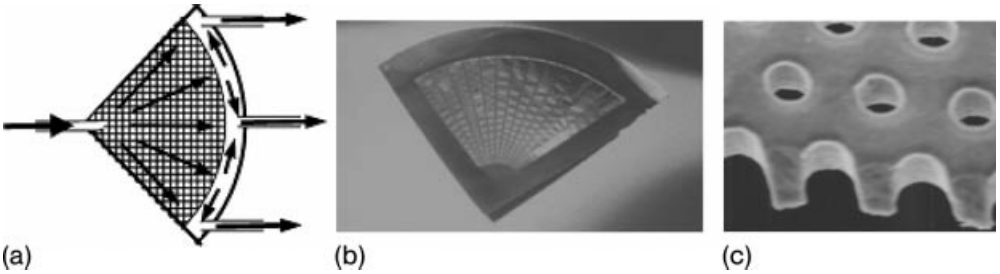

Figure 12.9 Quadrant manifold channel with mesh (a) and photographs of complete nickel mesh (b) and mesh pore (c). Reproduced by permission of the Royal Society of Chemistry [31].

The extracted phenol concentration in water is near the equilibrium value for a wide range of total volume flow rates. Both mixers require a contact time of less than 1 s to reach the equilibrium concentration.

Another type of microstructured device for generating dispersions is a channel including micromeshes as shown in Figure 12.9 [31]. Micromeshes with pore diameter, depth and spacing each of $\sim 5\,\mu m$ are formed by electrodeposition of nickel on substrates with defined photoresist layers.

Sprogies *et al.* compared micromixers for use in extractions based on emulsions [32]. They revealed that a multilamination mixer is more efficient than a simple T-junction, whereas a nozzle-type mixer and a split-and-recombine mixer show the best results for emulsification and thus for extraction.

12.3.2
Coalescence of Droplets in Dispersions

Droplets in emulsions have large specific interfacial areas for mass transfer, but they are often difficult to break once formed. In most cases, the phases must be separated after the phase transfer processes. To overcome this disadvantage, the system consists of a small, magnetically stirred vessel ($300\,\mu L$) for extraction and an electrocoalescence device after this vessel was developed (Figure 12.10) [33]. Phenol

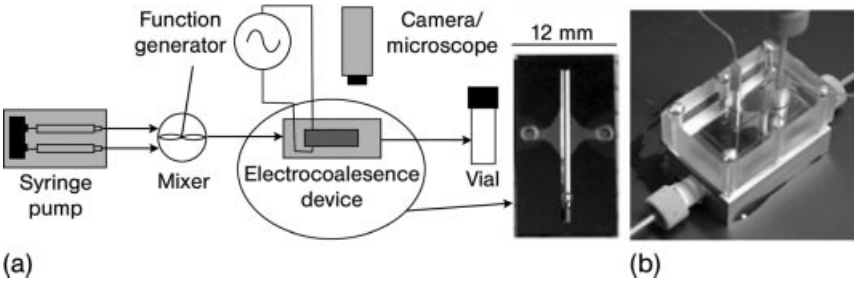

Figure 12.10 Schematic of the system for extraction and emulsion coalescence (a) and photograph of emulsion coalescence device (b). Reproduced by permission of the Royal Society of Chemistry [33].

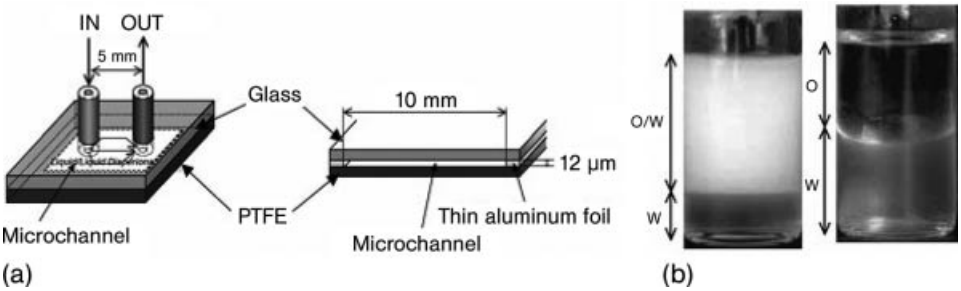

Figure 12.11 Schematic of the device for emulsion coalescence (a) and photograph of dispersion before and after flowing the device (b). Reproduced by permission of Elsevier [34].

and *p*-nitrophenol from an aqueous to hexane–surfactant (Span 80) solution served as model systems. In addition to the increased surface area in the emulsion, the extraction efficiency is enhanced by reverse micelles resulting from the presence of surfactants. The channel dimensions of electrocoalescence device are 20 mm long, 650 μm deep and 100 μm wide at the bottom and 970 μm wide at the top. Increasing the applied potential beyond 6 V leads to rapid coalescence with large droplets.

A microchannel device for coalescing dispersed droplets without external energy supply has also been developed (Figure 12.11) [34]. The microchannel of this device consists of two flat plates made of glass and PTFE and its cross-section is rectangular. This device has the following features: (1) the dispersed droplets are deformed in the planar microchannel with rectangular cross-section and the liquid–liquid interface destabilizes; and (2) the interaction between the PTFE wall and the organic phase has a large influence on the continuous phase in the microchannel and a velocity difference between the continuous and dispersed phases is brought about. A stable liquid–liquid dispersion made from heptane and hexane as the dispersed phase and a 1.0 wt% sodium dodecyl sulfate aqueous solution as the continuous phase was supplied to this microchannel device (channel depth 5 μm) at a rate of 0.3 mL min^{-1}. As shown in Figure 12.11b, good liquid–liquid separation is attained continuously with a contact time shorter than 0.1 s and visible dispersed droplets barely exist in the exit liquid.

12.3.3
Precise Operation of Individual Droplets

In the previous examples of extraction using emulsion, droplets cannot be manipulated individually. Precisely designed droplets with a controlled extraction rate are necessary to control the ratio of reaction rate to mass transfer rate and useful for quantitative analysis and biotechnology. Controlling this ratio leads to the removal of intermediate desired products and avoidance of byproduct through consecutive or parallel reactions, resulting in an increase in the desired product selectivity. Owing to the ordered laminar flow and dominant effect of surface tension, droplets including a small volume of liquid (~nL–pL) can be precisely manipulated or trapped in a certain part of the channel by making a recess structure. This allows the control of the place

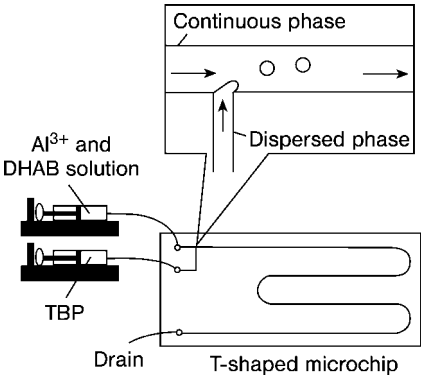

Figure 12.12 T-shaped channel to generate droplets for extraction. Reproduced by permission of Elsevier [39].

for performing extraction in a microstructured device. The relation between channel geometry, fluid operation and generated droplet sizes and pumping methods of immiscible fluids have been studied extensively [35–38].

Kumemura and Korenaga demonstrated the extraction of aluminum in a continuous phase extracted with 2,2-dihydroxyazobenzene (DHAB) as a metal chelate (Al^{3+}–DHAB) from buffer solution to tributyl phosphate (TBP, dispersed phase) [39]. As shown in Figure 12.12, a T-shaped channel 600 μm wide and 200 μm deep in the continuous phase and 70 μm wide and 20 μm deep in the dispersed phase is used for the extraction. The device is made of Pyrex glass. Using this device, the droplet volume can be controlled in the range 0.6–32 nL. The extraction time is 1 s, which is 90 times shorter than that of a conventional extraction method using a separating funnel. The overall mass transfer coefficient is estimated to be $57 \times 10^{-4}\,\mathrm{mm\,s^{-1}}$ with 0.6 nL droplets.

Chen *et al.* fabricated a glass microchannel with a rectangular recess for trapping organic droplets [40]. They demonstrated the extraction of butyl-Rhodamine B (BRB) in aqueous solution into 1-hexanol. Figure 12.13 shows the structure of the device.

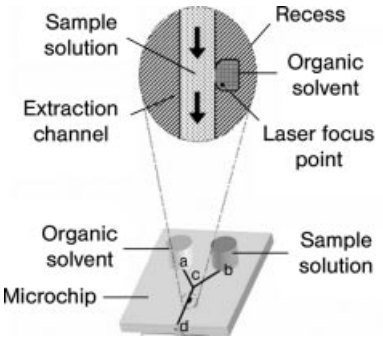

Figure 12.13 Extraction device with a square recess for trapping droplets. Reproduced by permission of the Royal Society of Chemistry [40].

The channel dimensions for sample solution (a–c) and organic solvent (b–c) are 5 mm long, 25 μm deep and 150 μm wide. The extraction channel (c–d) is 10 mm long, 25 μm deep and 250 μm wide. The recess structure has dimensions of 150 mm long, 100 μm wide and 25 μm deep, with a shrunken opening of 50 μm width. The extraction is performed by first adding 1 mL of organic solvent to the solvent reservoir on a clean, dry chip, keeping the sample reservoir empty. The solvent rapidly fills all the channels, including the recess, reaching the outlet of the extraction channel. Then the sample reservoir is filled with 100 mL of aqueous sample containing BRB, which produces a hydraulic pressure of 5 mmH_2O. The organic solvent is rinsed out of the extraction channel with the aqueous sample solution, leaving the organic drops trapped in the recess. Keeping the sample solution flowing continuously, BRB is transferred from the aqueous phase into the droplet through molecular diffusion. The combined effects of phase transfer of solute from an aqueous sample into an organic droplet and dissolution of the droplet into a by-passing aqueous stream can be exploited to produce high enrichment factors of about 5000, much higher than those achievable under macro-batch conditions. This device is useful for the *in situ* determination of a solute with a precisely controlled sample volume.

Other devices for extraction with trapping of droplets using an ultrasonic nanoliter liquid droplet ejector [41] and multiple opening rectangular recesses [42] have also been developed. As another method of trapping fluids, Sun *et al.* developed a microstructured device for extraction with stopped-flow manipulation [43].

12.4 Liquid–Liquid Slug Flow

As described above, extraction based on parallel flow is driven only by molecular diffusion. For achieving rapid extraction, a fairly narrow channel is needed, which leads to a high pressure drop in the channel. Extraction based on emulsions also has the drawback of difficulty in separating immiscible phases after extraction. Therefore, another fluid operation in microstructured devices for extraction avoiding these disadvantages has been pursued. Laminar flow in microchannels also permits the easy formation of liquid–liquid slug flow using a union tee as shown in Figure 12.14. Since slugs in the channel move like a periodic plug flow, a narrow residence time distribution can be achieved precisely [44, 45]. Internal circulation flow in the slug

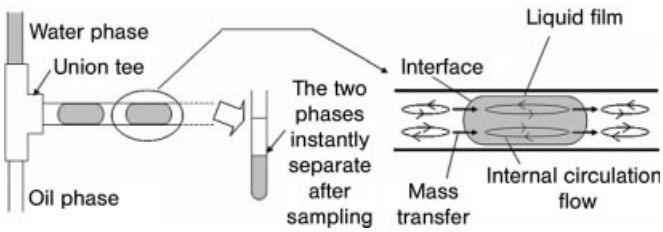

Figure 12.14 Internal circulation flow and mass transfer in slug flow formed using a union tee.

derived from the friction between the channel wall and the fluid in the slug due to a high surface area-to-volume ratio is expected to enhance the performance of mixing, which is mainly driven by molecular diffusion in laminar flow [46, 47]. The circulation flow also enhances mass transfer between the slugs of the two phases, since the concentration near the interface is renewed by the flow [48]. In other words, the concentration of the extract can be controlled through the internal circulation in each slug. The liquid film formed between the reactor wall and droplet phase increases the area of the active interface between the two phases, leading to improved mass transfer. Hence liquid–liquid slug flow can be used for rapid extraction. In addition, the two phases can be easily separated after the extraction using liquid–liquid slug flow, since the slug size is several tens times larger than the droplet size in the emulsion. Therefore, extraction in liquid–liquid slug flow is expected to be effective for the entire extraction process. In this section, devices integrated into the extraction process are first considered. Second, instances of the quantitative analysis of mass transfer in slug flow are reviewed. Then, we introduce the application of extraction based on slug flow to organic syntheses.

12.4.1
Extraction Process Based on Slug Flow

Aoki *et al.* investigated the effectiveness of slug flow in a narrow channel for the extraction of phenol from dodecane to water [49]. The experimental method for extraction based on slug flow is as follows. Distilled water and 1000 ppm phenol–dodecane were fed to an i.d. 1.3 mm, 1/16 inch union tee through silicon tubes with i.d. 1.0 mm and length 1.0 m. PTFE tubes with i.d. 0.8 mm with lengths calculated based on the residence time and total flow rates were attached to the outlet of the tees. The ratio of phenol–dodecane flow rate to total flow rate, w_0, was 0.5. The slug lengths of the two phases were measured with a ruler. Both phases were collected in a test-tube for 45 s. The two phases separated right after sampling. For comparison, C_w obtained by only contacting dodecane and the water phase for 45 s in a test-tube was also measured.

Figure 12.15 shows the effect of total flow rate V_t on C_w and the average slug length of the two phases. The results indicate that the increase in total flow rate improved the concentration of extracted phenol. This is because the circulation rate in the slugs was

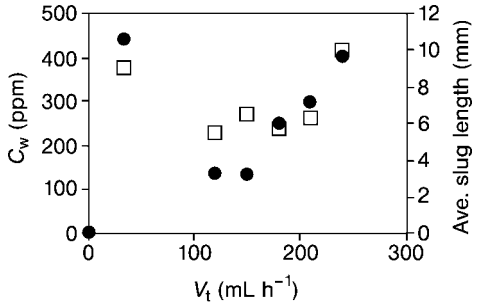

Figure 12.15 C_w and slug length as a function of total volume flow rate.

Table 12.2 Comparison of operation times for extraction and two phase separation.

Extraction based on	Extraction time (s)	Two phase separation time
Slug flow	~10	Instantaneous
Emulsion	~1	~Hours

enhanced with increasing V_t. No extraction occurred when the phases were contacted only in the test-tube ($V_t = 0\,\mathrm{mL\,h^{-1}}$ and without circulation flow). This also indicates that mass transfer occurs only in the outlet tube when slug flow is formed. Thus, rapid internal circulation flow enhances the extraction efficiency.

Aoki *et al.* [49] also compared extraction based on slug flow and that based on emulsion generated by a micromixer from the viewpoint of the total operation time for extraction and separation of the two phases. Table 12.2 summarizes the scale of operation time of extraction and the two-phase separation for the two extraction methods. For the extraction based on slug flow, the water and oil phases are separated right after sampling in the test-tube. For this reason, the total operation time for extraction and two phase separation is approximately equal to the time for extraction. Although the extraction time for emulsion is shorter than that for slug flow, the extraction based on emulsion requires an additional operation such as centrifugation and a longer total operation time for extraction itself and two-phase separation.

Using the easy separation of immiscible fluids at the exit of slug flow, a continuous system in which a phase separator (Figure 12.16) is connected right after an extractor has been developed [50]. The phase separator is fabricated in polycarbonate, 0.1–1 mm pore PTFE membrane. The channel sizes are 0.5 mm width and depth and 20 mm length. The organic phase wets the hydrophobic membrane and is driven through the membrane pores by the imposed pressure difference, leaving the aqueous solution behind in the top portion of the device. This device is especially useful for multistep synthesis including continuous microchemical separation. Extraction and separation of the two phases can also be performed in a short time in one continuous channel with branched hydrophobic and hydrophilic outlets.

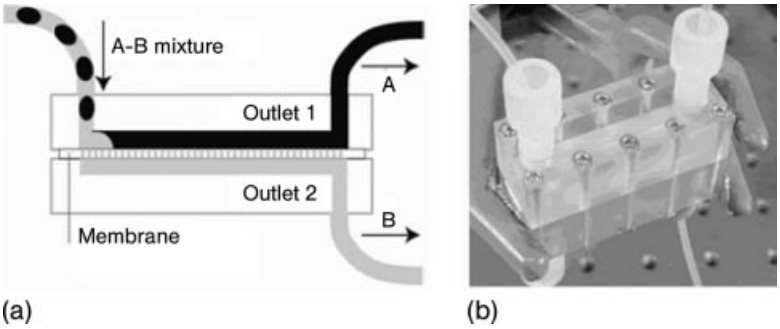

Figure 12.16 Schematic (a) and photograph (b) of phase separator. Reproduced by permission of the Royal Society of Chemistry [50].

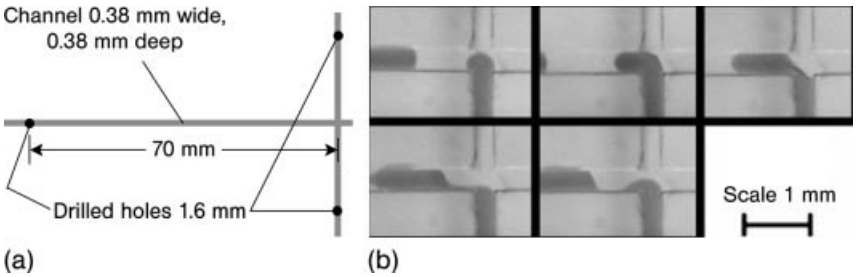

Figure 12.17 Cross channel for extraction using slug flow (a) and formed slugs (b). Reproduced by permission of the Royal Society of Chemistry [48].

12.4.2
Quantitative Study of Mass Transfer in Slug Flow

Mass transfer in slug flow has been quantitatively studied. Burns and Ramshaw formed slug flow using a soda-lime glass cross channel as shown in Figure 12.17 [48]. Acetic acid in an organic phase comprised of silicone oil and kerosene moves into an aqueous phase including KOH or NaOH with neutralization. Values of the mass transfer coefficient k are obtained from the experimental data using the following equation:

$$dC/dt = ka\Delta C \tag{12.1}$$

where ΔC is the difference in concentration of acetic acid between the organic and aqueous slugs, a is the specific surface area and t is the time. The coefficients are found to be in the range 0.16–0.56 mm s^{-1}, with higher values being obtained for higher flow velocities where internal convection should be greater. The authors also compared the mass transfer rate of acetic acid with slug flow and that with only molecular diffusion. The mass transfer rate between the two phases corresponds to a diffusive process with a path of between 110 and 200 μm, which is shorter than the channel width of 380 μm.

Kashid *et al.* studied the flow patterns within the slugs and mass transfer between two consecutive slugs in liquid–liquid slug flow using a finite element-based computational fluid dynamics (CFD) model [51]. The model equations are implemented in the open-source software FEATFLOW (www.featflow.de). Figure 12.18 shows snapshots of the concentration profiles of the extract (acetic acid). These results are compared with experimental results and are consistent with them.

12.4.3
Application of Mass Transfer in Slug Flow to Organic Synthesis

Enhanced mass transfer by internal circulation flow in slug flow can also be used in biphasic reactions. Owing to many operating parameters such as flow rate, volume ratio of two phases and channel diameter that can be adjusted flexibly in slug flow, the

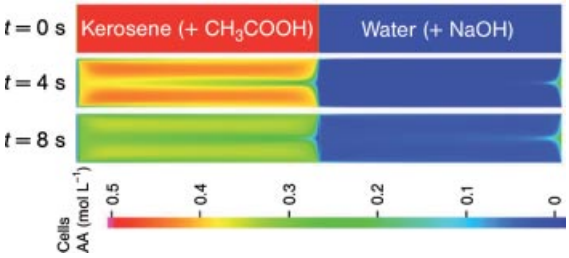

Figure 12.18 Concentration profiles of acetic acid in two consecutive slugs with various operation times t (slug length = 1.9 mm, slug velocity = 3.33 m s^{-1}). Reproduced by permission of Elsevier [51].

mixing rate of reactants and the mass transfer rate have the possibility of being controlled separately, which leads to improved selectivity of the desired products.

Ahmed-Omer *et al.* compared the yields of *p*-nitrophenolate produced through the hydrolysis of *p*-nitrophenyl acetate for slug flow, parallel flow and batch operation (flask with stirring) [52]. The reactants of this reaction, *p*-nitrophenyl acetate in toluene and aqueous sodium hydroxide, form two phases. Once the acetate has been hydrolyzed, the *p*-nitrophenolate transfers into the aqueous phase. The hydrolysis is a fast reaction and the rate is controlled by molecular diffusion. A V-inlet junction (width 150 µm and depth 300 µm) was used for parallel flow and a T-inlet junction (width 300 µm and depth 300 µm) was employed for slug flow. Both junctions are connected to a microchannel of 300 µm depth, 300 µm width and 400 mm length. The material of the whole microchannel is poly(methyl methacrylate) (PMMA). The common reaction temperature is 20 °C. As shown in Figure 12.19, for the same

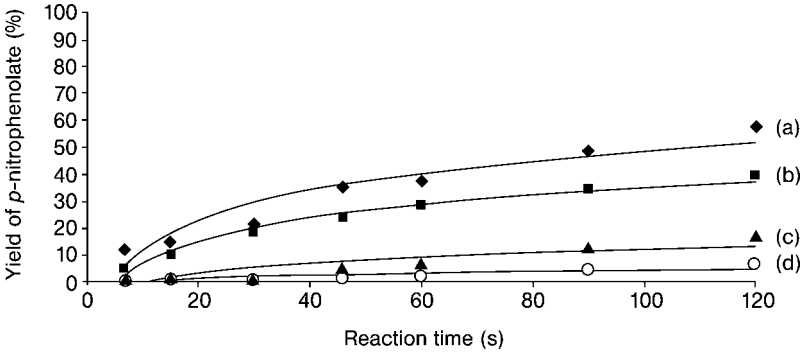

Figure 12.19 Comparison of the yields of *p*-nitrophenolate: (a) segmented flow (organic phase: toluene); (b) parallel flow [organic phase: acetonitrile–toluene (1:1)]; (c) hydrolysis reaction in a flask with stirring [organic phase: acetonitrile–toluene (1:1)]; (d) hydrolysis reaction in a flask with stirring (organic phase: toluene). Reproduced by permission of Elsevier [52].

reaction time, slug flow gives the highest yield of *p*-nitrophenolate and parallel flow the second highest. This result shows that slug flow greatly improves mass transfer between immiscible fluids.

Another instance of the extended use of slug flow in biphasic reactions are the nitration of a single-ring aromatic compound [53]. The reactor is a Y-piece mixing element, with an angle of 120° between the uniform cylindrical inlet channels of i.d. 0.5–1.0 mm with a PTFE capillary (i.d. 0.5–1.0 mm) attached directly downstream of the Y-piece. The capillary is surrounded by a thermostated jacket with constant temperature of 60 or 120 °C. In addition to enhanced mass transfer between immiscible fluids, the heat liberated by the nitration, which is a strongly exothermic reaction, is removed very effectively owing to the excellent heat transfer, which is mainly due to the small capillary dimensions and the resulting high specific surface area. The nitration of the aromatic can therefore be performed under isothermal conditions. These precisely controlled reaction conditions result in an enhanced yield of mononitrated product and avoidance of dinitrated byproducts via consecutive reactions and phenolic byproducts via parallel reactions.

Slug flow can also be used for reaction systems with phase transfer catalysis. Okamoto demonstrated the synthesis of 2-ethylmalonic acid dimethyl ester [$C_2H_5CH(COOCH_3)_2$] from iodoethane (C_2H_5I) and malonic acid dimethyl ester [$CH_2(COOCH_3)_2$] in CH_2Cl_2 phase using a phase-transfer catalysis, tetrabutylammonium hydrogensulfate, with NaOH in the aqueous phase [54]. Slug flow is formed by alternating pumping of CH_2Cl_2 and water phase. The reactor is a glass tube of i.d. 0.5 mm and o.d. 6 mm immersed in a water-bath (32.5 °C). The result shows that a short slug gives a higher yield of the product than a long slug and batchwise operation.

12.5 Conclusion

Microstructured devices for extraction divided into three groups according to fluid operations have been reviewed. The advantages and disadvantages of the device for each fluid operation are summarized in Table 12.3. Although several extraction devices allowing effective separation have been developed, a way to choose a device to match a certain objective of production is required. Design guidelines for choosing which fluid operation type of device and for determining the optimum device dimensions and operation condition according to production goal are expected to be developed. These guidelines will lead to the establishment of an extraction and reaction process with precisely controlled extraction rate and increased desired product selectivity.

The microstructured extraction devices are attractive for process intensification, since they allow precisely controlled and rapid extraction and the small dimensions permit their flexible use in multiple-stage processes including the repetition of reaction and extraction operations. These advantages are effective for reaction

Table 12.3 Advantages and disadvantages of microfluidic devices for extraction for each fluid operation.

Flow pattern	Advantage	Disadvantage
Parallel flow	Instant separation of immiscible phase after extraction	Rapid extraction requires narrow channel, which leads to high pressure drop in microchannel
Emulsion	Rapid separation due to fairly large specific surface area	Difficulty in phase separation after extraction
Individual droplet manipulation	Precise operation of single droplets	Not suitable for high-throughput operation
Slug flow	Rapid extraction due to internal circulation flow, instantaneous separation of immiscible phase after extraction	Limited operating conditions to form slug flow

processes including fast reactions and on-site purification of domestic and industrial drainage, which requires a novel separation technique that has not yet been established.

References

1 T. Minagawa, M. Tokeshi, T. Kitamori, Integration of a wet analysis system on a glass chip: determination of Co(II) as 2-nitroso-1-naphthol chelates by solvent extraction and thermal lens microscopy. *Lab Chip*, **2001**, *1*, 72–75.

2 P. Kuban, J. Berg, P. K. Dasgupta, Vertically stratified flows in microchannels. computational simulations and applications to solvent extraction and ion exchange. *Anal. Chem.*, **2003**, *75*, 3549–3556.

3 M. Tokeshi, T. Minagawa, T. Kitamori, Integration of a microextraction system on a glass chip: ion-pair solvent extraction of Fe(II) with 4,7-diphenyl-1,10-phenanthrolinedisulfonic acid and tri-*n*-octylmethylammonium chloride. *Anal. Chem.*, **2000**, *72*, 1711–1714.

4 H. Hisamoto, T. Horiuchi, M. Tokeshi, A. Hibara, T. Kitamori, On-chip integration of neutral ionophore-based ion pair extraction reaction. *Anal. Chem.*, **2001**, *73*, 1382–1386.

5 P. Žnidaršič-Plazl, I. Plazl, Steroid extraction in a microchannel system – mathematical modelling and experiments. *Lab Chip*, **2007**, *7*, 883–889.

6 S. A. Bowden, P. B. Monaghan, R. Wilson, J. Parnell, J. M. Cooper, The liquid–liquid diffusive extraction of hydrocarbons from a North Sea oil using a microfluidic format, *Lab Chip*, **2006**, *6*, 740–743.

7 H. Hotokezaka, M. Tokeshi, M. Harada, T. Kitamori, Y. Ikeda, Development of the innovative nuclide separation system for high-level radioactive waste using microchannel chip – extraction behavior of metal ions from aqueous phase to organic phase in microchannel. *Prog. Nucl. Energy*, **2005**, *47*, 439–447.

8 H. B. Kim, K. Ueno, M. Chiba, O. Kogi and N. Kitamura, Spatially-resolved fluorescence spectroscopic study on liquid/liquid extraction processes in polymer microchannels. *Anal. Sci.*, **2000**, *16*, 871–876.

9 M. Tokeshi, T. Minagawa, T. Kitamori, Integration of a microextraction system: Solvent extraction of a Co–2-nitroso–5-dimethylaminophenol complex on a microchip. *J. Chromatogr. A*, **2000**, *894*, 19–23.

10 Z. Cai, Q. Fang, H. Chen, Z. Fang, A microfluidic chip based liquid–liquid extraction system with microporous membrane. *Anal. Chim. Acta*, **2006**, *556*, 151–156.

11 X. Wang, C. Saridara, S. Mitra, Microfluidic supported liquid membrane extraction. *Anal. Chim. Acta*, **2005**, *543*, 92–98.

12 A. Hibara, M. Tokeshi, K. Uchiyama, H. Hisamoto, T. Kitamori, Integrated multilayer flow system on a microchip. *Anal. Sci.*, **2001**, *17*, 89–93.

13 M. Surmeian, M. N. Slyadnev, H. Hisamoto, A. Hibara, K. Uchiyama, T. Kitamori, Three-layer flow membrane system on a microchip for investigation of molecular transport. *Anal. Chem.*, **2002**, *74*, 2014–2020.

14 A. Hibara, M. Nonaka, H. Hisamoto, K. Uchiyama, Y. Kikutani, M. Tokeshi, T. Kitamori, Stabilization of liquid interface and control of two-phase confluence and separation in glass microchips by utilizing octadecylsilane modification of microchannels. *Anal. Chem.*, **2002**, *74*, 1724–1728.

15 H. Xiao, D. Liang, G. Liu, M. Guo, W. Xing, J. Cheng, Initial study of two-phase laminar flow extraction chip for sample preparation for gas chromatography. *Lab Chip*, **2006**, *6*, 1067–1072.

16 T. Maruyama, T. Kaji, T. Ohkawa, K.-I. Sotowa, H. Matsushita, F. Kubota, N. Kamiya, K. Kusakabe, M. Goto, Intermittent partition walls promote solvent extraction of metal ions in a microfluidic device. *Analyst*, **2004**, *129*, 1008–1013.

17 T. Tagawa, S. Aljbour, M. Matouq, H. Yamada, Micro-channel reactor with guideline structure for organic–aqueous binary system. *Chem. Eng. Sci.*, **2007**, *62*, 5123–5126.

18 T. Maruyama, H. Matsushita, J. Uchida, F. Kubota, N. Kamiya, M. Goto, Liquid membrane operations in a microfluidic device for selective separation of metal ions. *Anal. Chem.*, **2004**, *76*, 4495–4500.

19 H. Miyaguchi, M. Tokeshi, Y. Kikutani, A. Hibara, H. Inoue, T. Kitamori, Microchip-based liquid–liquid extraction for gas-chromatography analysis of amphetamine-type stimulants in urine. *J. Chromatogr. A*, **2006**, *1129*, 105–110.

20 E. L. Paul, V. A. Atiemo-Obeng, S. M. Kresta. *Handbook of Industrial Mixing: Science and Practice*, John Wiley & Sons, Inc. Hoboken, NJ, **2004**, p. 33.

21 H. Hisamoto, T. Saito, M. Tokeshi, A. Hibara, T. Kitamori, Fast and high conversion phase-transfer synthesis exploiting the liquid–liquid interface formed in a microchannel chip. *Chem. Commun.*, **2001**, 2662–2663.

22 T. Maruyama, J. Uchida, T. Ohkawa, T. Futami, K. Katayama, K. Nishizawa, K. -I. Sotowa, F. Kubota, N. Kamiyaa, M. Goto, Enzymatic degradation of *p*-chlorophenol in a two-phase flow microchannel system. *Lab Chip* **2003**, *3*, 308–312.

23 J. R. Bourn, O. M. Kut, J. Lenzner, H. Maire, Kinetics of the diazo coupling between 1-naphthol and diazotized sulfanilic acid. *Ind. Eng. Chem. Res.*, **1990**, *29*, 1761–1765.

24 M. Tokeshi, T. Minagaqwa, K. Uchiyama, A. Hibara, K. Sato, H. Hisamoto, T. Kitamori, Continuous-flow chemical processing on a microchip by combining microunit operations and a multiphase flow network. *Anal. Chem.*, **2002**, *74*, 1565–1571.

25 M. Tokeshi, T. Kitamori, Continuous flow chemical processing on a microchip using microunit operations and a multiphase flow network. *Prog. Nucl. Energy* **2005**, *47*, 434–438.

26 T. Honda, M. Miyazaki, Y. Yamaguchi, H. Nakamura, H. Maeda, Integrated

microreaction system for optical resolution of racemic amino acids. *Lab Chip* **2007**, *7*, 366–372.

27 H. Pennemann, S. Hardt, V. Hessel, P. Löb, F. Weise, Micromixer based liquid/liquid dispersion. *Chem. Eng. Technol.*, **2005**, *28*, 501–508.

28 P. Löb, H. Pennemann, V. Hessel, Y. Men, Impact of fluid path geometry and operating parameters on l/l-dispersion in interdigital micromixers. *Chem. Eng. Sci.*, **2006**, *61*, 2959–2967.

29 K. Benz, K. -P. Jäckel, K. -J. Regenauer, J. Schiewe, K. Drese, W. Ehrfeld, V. Hessel, H. Löwe, Utilization of micromixers for extraction processes. *Chem. Eng. Technol.*, **2001**, *24*, 11–17.

30 K. Mae, T. Maki, I. Hasegawa, U. Eto, Y. Mizutani, N. Honda, Development of a new micromixer based on split/recombination for mass production and its application to soap free emulsifier. *Chem. Eng. J.*, **2004**, *101*, 31–38.

31 D. A. Wenn, J. E. A. Shaw, B. Mackenzie, A mesh microcontactor for 2-phase reactions. *Lab Chip*, **2003**, *3*, 180–186.

32 T. Sprogies, J. M. Köhler, G. A. Gross, Evaluation of static micro mixers for flow-through extraction by emulsification. *Chem. Eng. J.*, **2007**, *35*, 199–202.

33 J. G. Kralj, M. A. Schmidt, K. F. Jensen, Surfactant-enhanced liquid–liquid extraction in microfluidic channels with inline electric-field enhanced coalescence. *Lab Chip* **2005**, *5*, 531–535.

34 Y. Okubo, M. Toma, H. Ueda, T. Maki and K. Mae, Microchannel devices for the coalescence of dispersed droplets produced for use in rapid extraction process. *Chem. Eng. J.*, **2004**, *101*, 39–48.

35 J. M. Köhler, Th. Henkel, A. Grodrian, Th. Kirner, M. Roth, K. Martin, J. Metze, Digital reaction technology by micro segmented flow – components, concepts and applications. *Chem. Eng. J.*, **2004**, *101*, 201–216.

36 D. R. Link, S. L. Anna, D. A. Weitz, H. A. Stone, Geometrically mediated breakup of drops in microfluidic devices. *Phys. Rev. Lett.*, **2004**, *92*, 054503.

37 T. Nisisako, T. Torii, T. Higuchi, Droplet formation in a microchannel network. *Lab Chip* **2002**, *2*, 24–26.

38 T. S. Sammarco, M. A. Burns, Thermocapillary pumping of discrete drops in microfabricated analysis devices. *AIChE J.*, **1999**, *45*, 350–366.

39 M. Kumemura, T. Korenaga, Quantitative extraction using flowing nano-liter droplet in microfluidic system. *Anal. Chim. Acta*, **2006**, *558*, 75–79.

40 H. Chen, Q. Fang, X.-F. Yin, Z.-L. Fang, Microfluidic chip-based liquid–liquid extraction and preconcentration using a subnanoliter-droplet trapping technique. *Lab Chip*, **2005**, *5*, 719–725.

41 H. Yu, J. W. Kwon, E. S. Ki, Chembio extraction on a chip by nanoliter droplet ejection. *Lab Chip*, **2005**, *5*, 344–349.

42 H. Shen, Q. Fang, Z.-L. Fang, A microfluidic chip based sequential injection system with trapped droplet liquid–liquid extraction and chemiluminescence detection. *Lab Chip*, **2006**, *6*, 1387–1389.

43 M. Sun, W.-B. Du, Q. Fang, Microfluidic liquid–liquid extraction system based on stopped-flow technique and liquid core waveguide capillary. *Talanta*, *70*, **2006**, 392–396.

44 H. Song, J. D. Tice, R. F. Ismagilov, A microfluidic system for controlling reaction networks in time. *Angew. Chem. Int. Ed.*, **2003**, *42*, 768–772.

45 F. Trachsel, A. Günther, S. Khan, K. F. Jensen, Measurement of residence time distribution in microfluidic systems. *Chem. Eng. Sci.*, **2005**, *60*, 5729–5737.

46 M. N. Kashid, I. Gerlach, S. Goetz, J. Franzke, J. F. Acker, F. Platte, D. W. Agar, S. Turek, Internal circulation within the liquid slugs of a liquid–liquid slug-flow capillary microreactor. *Ind. Eng. Chem. Res.*, *44*, **2005**, 5003–5010.

47 W. Tanthapanichakoon, N. Aoki, K. Matsuyama, K. Mae, Design of mixing in microfluidic liquid slugs based on a new

dimensionless number for precise reaction and mixing operations. *Chem. Eng. Sci.*, **2006**, *61*, 4220–4232.

48 J. C. Burns, C. Ramshaw, The intensification of rapid reactions in multiphase systems using slug flow in capillaries. *Lab Chip*, **2001**, *1*, 10–15.

49 N. Aoki, T. H. Khoo, Y. Okubo, K. Mae, Enhanced mass transfer by liquid–liquid slug flow in microchannels for efficient extraction, in *Proceedings of AIChE 2007 Spring Meeting*, 22–26 April 2007, Houston, TX, **2007**, Paper 89d.

50 J. G. Kralj, H. R. Sahoo, Klavs F. Jensen, Integrated continuous microfluidic liquid–liquid extraction. *Lab Chip*, **2007**, *7*, 256–263.

51 M. N. Kashid, D. W. Agar, S. Turek, CFD modelling of mass transfer with and without chemical reaction in the liquid–liquid slug flow microreactor. *Chem. Eng. Sci.*, **2007**, *62*, 5102–5109.

52 B. Ahmed-Omer, D. Barrow, T. Wirth, Effect of segmented fluid flow, sonication and phase transfer catalysis on biphasic reactions in capillary microreactors. *Chem. Eng. J.*, **2007**, *135* 280–283.

53 G. Dummann, U. Quittmann, L. Gröschel, D. W. Agar, O. Wörz, K. Morgenschweis, The capillary-microreactor: a new reactor concept for the intensification of heat and mass transfer in liquid–liquid reactions. *Catal. Today*, **2003**, *79–80*, 433–439.

54 H. Okamoto, Effect of alternating pumping of two reactants into a microchannel on a phase transfer reaction. *Chem. Eng. Technol.*, **2006**, *29*, 504–506.